

---

# 6

## Equatorial Currents: Observations and Theory

*Ants Leetmaa  
Julian P. McCreary, Jr.  
Dennis W. Moore*

### 6.1 Introduction

Historically, our knowledge of the circulation patterns in the tropics was derived from compilations of ship-drift data and so was restricted to a description of the surface currents. Although information of this type is crude, a picture of the spatial and temporal structure of the surface flow field was deduced over the years, and it has been little improved upon in the modern era of instrumentation. By contrast, almost all of the information about subsurface equatorial flows has been acquired recently. It is remarkable that one of the major ocean currents, the Pacific Equatorial Undercurrent, was not discovered until 1952.

For many reasons, progress in understanding equatorial circulations has been slow. The equatorial regions are vast and remote. The swift currents and high vertical shears put special demands on instrumentation. The geostrophic approximation, which is so useful at mid-latitudes, breaks down close to the equator and cannot be relied on to give accurate information about the currents. Finally, the flows seem much more time dependent than at mid-latitudes. Hence, on the basis of individual cruises, haphazardly taken in time and space, it is difficult to develop a consistent picture of the circulation patterns.

The variability of equatorial circulations has only recently been appreciated. This is partly because a great deal of the information about equatorial circulations comes from the central Pacific, where historically the mean appears to dominate the transient circulation; recent NORPAX (North Pacific Experiment) observations (Wyrski, McLain, and Patzert, 1977; Patzert, Barnett, Sessions, and Kilonsky, 1978), however, suggest that the variability can be quite large even there. In other regions such as the western or eastern Pacific or the Indian Ocean, the fluctuating components are as large as or larger than the means.

The goal of this chapter is to give a short overview of the outstanding features of the equatorial ocean circulation patterns, the dominant spatial and temporal structures of the Pacific equatorial wind field (as an example of the kinds of driving mechanisms that need to be considered), and a summary of some of the theoretical ideas that have been developed to explain the ocean circulation and its relation to the wind field. No attempt is made to be comprehensive because in recent years there have been numerous excellent reviews of equatorial phenomena and theories for them. These include articles by Knauss (1963), Tsuchiya (1970), Rot-schi (1970), Philander (1973), Gill (1975a), and Moore and Philander (1977). A collection of papers discussing various topics of equatorial oceanography is contained in the proceedings of the FINE (1978) workshop, held

at Scripps Institution of Oceanography during the summer of 1977. A comprehensive discussion of analytic techniques for studying forced baroclinic ocean motions in the equatorial regions is presented in a three-part paper by Cane and Sarachik (1976, 1977, 1979). In discussing the theories, we shall stress the important physical ideas of each model (avoiding whenever possible the use of mathematics), put them in historical perspective, and relate them to the observations. The objective here is to identify the observations for which we have physical theories, and thereby indicate where further work is needed.

The importance of knowing the detailed time and spatial structure of the wind field is emphasized throughout this chapter. The reason is that in the tropics, the characteristic response times for baroclinic oceanic processes are much shorter than they are at mid-latitude and are much closer to the time scales characterizing the wind variations. Therefore the baroclinic response to atmospheric forcing is expected to be much stronger than at mid-latitude. The implication is that in order to arrive at a satisfactory explanation of the oceanic features, the temporal and spatial structure of the atmospheric forcing must be known accurately.

## 6.2 Observations

### 6.2.1 The Ocean

The surface currents are characterized by zonal bands in which the flow is alternately eastward or westward (Knauss, 1963). The eastward flows are referred to as *countercurrents* because they flow counter to the direction of the easterly trade winds. The westward flows are referred to as *North and South Equatorial Currents*. In the Atlantic and the Pacific, the North Equatorial Countercurrent (NECC) is approximately located between 5° and 10°N with westward flow to the north of this region in the North Equatorial Current (NEC) and westward flow to the south of it in the South Equatorial Current (SEC). There is also evidence for a South Equatorial Countercurrent (SECC) in both oceans between 5 and 10°S (Reid, 1964b; Tsuchiya, 1970; Merle, 1977); these flows are not as well developed, however, as the NECC. Both the intensity and location of the various currents vary seasonally (Knauss, 1963; Merle, 1977). The SEC and NECC are strongest during July and August. In the northern winter and spring the SEC generally vanishes and the NECC is weak; in the eastern Pacific there is some evidence that during this time the NECC is discontinuous at some longitudes or is entirely absent (Tsuchiya, 1974). In the northern summer the Pacific NECC assumes its northernmost position, whereas in the northern winter the current lies closest to the equator. The data base is insufficient to show an analogous migration of the Atlantic NECC.

The structure of the surface currents in the Indian Ocean differs markedly from those in the other two oceans (*African Pilot*, 1967). In the Indian Ocean the SEC usually lies totally south of 4°S. The predominantly eastward flow in the Indian Ocean is almost totally confined between the equator and the SEC. North of the equator the flow direction varies seasonally. During the northeast monsoon it is to the west.

The different circulation pattern in the Indian Ocean is no doubt related to the nature of the wind field. In the Atlantic and the Pacific, the southeast and the northeast trades are well developed over most of the ocean throughout the year. The mean stress is generally greater than the annual or semiannual components. In the Indian Ocean south of about 10°S, the southeast trades are reasonably steady. North of 10°S, the mean winds are weak and the stress field is dominated by the strong, regular forcing of the southwest and northeast monsoons.

The earliest measurements that indicated that the currents at depth might behave differently from those at the surface were made in 1886 by Buchanan (1888; see discussion by Montgomery and Stroup, 1962). Using drogues, he found that the subsurface flow on the equator in the Atlantic at 14°W was toward the southeast, while the surface flow had a slight westward set. These unusual measurements were thought not to be representative until after the discovery of the Equatorial Undercurrent in the Pacific in 1952 (Cromwell, Montgomery, and Stroup, 1954). The Equatorial Undercurrent has been found to be a subsurface eastward flow that is about 100–200 m thick and 200–300 km wide. It is centered approximately on the equator. Its core lies just beneath the base of the mixed layer in the top of the equatorial thermocline. Undercurrents are found in all three oceans. The one in the Indian Ocean, however, appears to be present primarily during the northeast monsoon, and most observations of it have been made during the spring. A thorough discussion of early evidence for the Equatorial Undercurrent in all three oceans is given in Montgomery (1962); see also Philander (1973).

Evidence for additional subsurface countercurrents in the Pacific is discussed in detail by Tsuchiya (1975). He finds narrow subsurface countercurrents in the Pacific Ocean symmetrically located about the equator. The jets occur at a depth of 200–300 m, and are associated with the poleward limits of the thermostat (a subsurface, relatively homogeneous layer of equatorial 14°C water). In the eastern Pacific, they are located roughly at 5°N and 5°S and are distinct from the surface countercurrents as well as from the Equatorial Undercurrent itself. Further to the west, the jets move closer to the equator (Taft and Kovala, 1979) and have been observed to merge with the Equatorial Undercurrent (Hisard, Merle, and Voituriez, 1970). The jets appear in

virtually all central and eastern Pacific Ocean hydrographic sections, and thus appear to be permanent features of the equatorial current system there. There is also evidence that similar currents exist in the Atlantic Ocean as well (Tsuchiya, 1975; Cochrane, Kelly, and Olling, 1979).

Although something is known about the temporal fluctuations of the surface currents from ship-drift observations, little systematic information exists about the time and space variations at any frequency. The recent survey article by Wunsch (1978b) discusses the observational evidence for equatorial motions with periods from a few days to several months. Fluctuations have been observed with periods of 4 to 5.5 days (Wunsch and Gill, 1976; Weisberg, Miller, Horigan, and Knauss, 1980; Weisberg, Horigan, and Colin, 1979) Harvey and Patzert (1976) present evidence that suggests waves with a period of about 25 days. Features with a similar time scale and wavelength of about 1000 km are observed in the satellite infrared images of the equatorial front by Legeckis (1977b). In the Atlantic, Düing et al. (1975) found evidence for a meandering of the Equatorial Undercurrent with a "period" of 2-3 weeks and a "wavelength" of 3200 km during GATE (GARP Atlantic Tropical Experiment).

Neumann, Beatty, and Escowitz (1975) and Katz et al. (1977) have shown that the east-west slope of the thermocline in the Atlantic varies on a seasonal time scale. This variation appears to be in phase with changes in the zonal component of the wind stress. When the trades are strongest the tilt of the thermocline is the greatest, and when the stress is at a minimum so is the slope. Meyers (1979), in a similar analysis for the Pacific, finds strong annual and interannual variations in the depth of the 14° isotherm. This isotherm was chosen because it is representative of movements of the thermocline as a whole. The east-west slope was a minimum in May and June and a maximum during October and November. The easterly wind stress is weakest in March-May; there is some phase change, however, in the annual component with longitude. Hence there appears to be a time lag between the minimum east-west slope and the minimum wind. The exact relation between the winds and the variations in the slope was difficult to deduce because the variations about the mean slope are small and because smaller spatial scales than the basin width were present in the slope of the 14° isotherm. These smaller scales appear to propagate westward. In the Indian Ocean the mean east-west stress is small. In the transition between the monsoons, however, westerly winds appear along most of the equator. Associated with these is an eastward oceanic jet and simultaneously a rise in the sea level off Sumatra and a rise of the thermocline off East Africa (Wyrtki, 1973a). The oceanic response appears to occur coincidentally with the winds.

## 6.2.2 The Wind Field

To date, most theoretical treatments of equatorial flows consider the applied wind stress to be some simple functions of time and latitude, whereas even the most general meteorological description of the trades indicates that there is considerable spatial and temporal structure (Riehl, 1954). In recent years, there have been several thorough analyses of the stress field over the ocean as derived from historical merchant-vessel reports. In the Pacific, this analysis was done for the whole ocean by Wyrtki and Meyers (1975) and for the eastern part by Hastenrath and Lamb (1977). The latter authors and Bunker (1976) also analyzed the winds over the tropical Atlantic. From these studies, it is possible to look in detail at the long-period temporal fluctuations and the large-scale spatial structure of the stress field. For the sake of brevity, we shall limit our discussion to the Pacific data. Some similar features are evident in the Atlantic, while the Indian Ocean wind field is dominated by the monsoon circulation.

Values of the zonal stress within 4° of the Pacific equator are shown in figure 6.1. These curves are derived from the mean monthly values of Wyrtki and

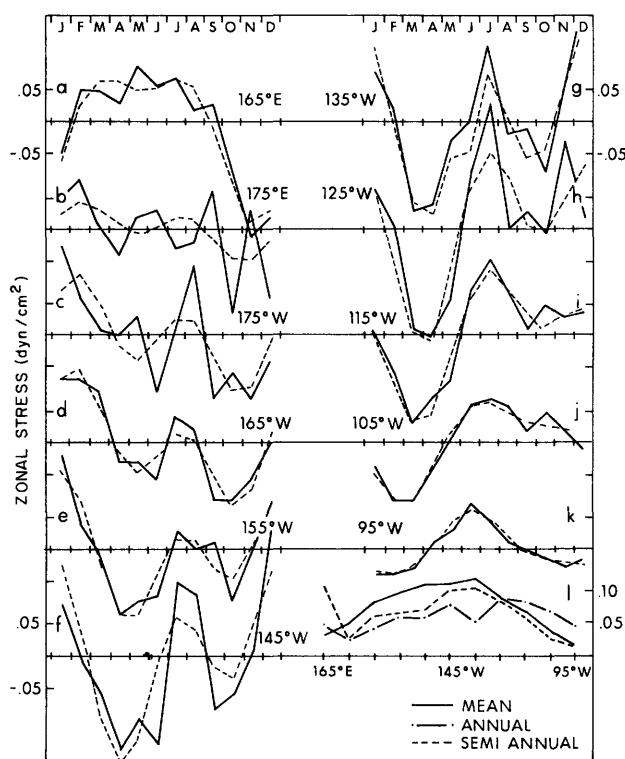


Figure 6.1 The monthly variation in the mean zonal stress between 4°N and 4°S. In figures 6.1a-6.1k, the solid curves display the average stress for blocks of 10° of longitude centered at the indicated values. The dashed curves show the proportion that is fitted by the annual and semiannual components. Figure 6.1l shows the amplitude of the mean, annual, and semiannual components as a function of longitude. The amplitude of the mean component has been reduced by a factor of five, i.e., at 145°W it is about 0.5 dyn cm<sup>-2</sup>.

Meyers (1975), which are tabulated for areas of 2° of latitude by 10° of longitude. The monthly values of the equatorial zonal stress with the yearly mean removed are shown in figures 6.1a–6.1k. As can be seen, the annual and semiannual components account for almost all of the annual variation. The amplitudes and phases of these components are tabulated in table 6.1. The phase of the annual component decreases rapidly, although irregularly, to the east. The phase of the semiannual component also decreases to the east, but more slowly. The amplitudes of the mean, annual, and semiannual components as a function of longitude are shown in figure 6.11. The mean stress over most of the Pacific is about a factor of five larger than the annual and semiannual components. The amplitude of each component varies strongly in the zonal direction. Thus we expect that models driven by zonally uniform stress distributions may not be adequate for describing the oceanic response to the wind.

Meyers (1979) presents evidence that the longitudinal structure of the wind field must be properly accounted for. He finds significant energy at the semiannual period in the eastern Pacific Ocean even though there is little energy in the wind stress there at that period. A study of the EASTROPAC data supports his findings. Figure 6.2 shows the average rate of change of the depth of the 20° isotherm (m/60 days) between 1°N and 1°S at four different longitudes. As can be seen, there is a pronounced semiannual variation, and the changes occur almost simultaneously at each longitude. The large amplitude of the changes (~50 m/60 days) is surprising considering the small amplitude of the semiannual component of the stress at these longitudes (0.02–0.03 dyn cm<sup>-2</sup>). We suggest that these fluctuations are caused by baroclinic waves that have propagated eastward from a region where the semiannual component of the stress is much larger. Meyers reached the same conclusion.

So far we have considered only winds in the vicinity of the equator and have ignored the transient changes in the stress, and the curl of the stress, that are related to seasonal movements of the Intertropical Convergence Zone (ITCZ). To investigate these effects, the monthly values of the stress averaged between 100 and 120°W were examined. To emphasize the meridional structure, the weak monthly mean stress at the equator (~0.1 dyn cm<sup>-2</sup>) was subtracted from the monthly mean value of the stress at each latitude. Resulting monthly values are shown in figure 6.3. The annual movement of the ITCZ has little effect close to the equator, with the largest amplitude of the variation in the stress occurring at about 9°N. There the amplitude is about 0.5 dyn cm<sup>-2</sup>. The variation south of the equator is considerably less. But it is evident that the annual variation in wind-stress curl can be very large and must be taken into account in the models.

Table 6.1 Amplitude and Phase of Annual and Semiannual Components of Zonal Stress<sup>a</sup>

	Annual		Semiannual	
	Amplitude (dyn cm <sup>-2</sup> )	Phase	Amplitude (dyn cm <sup>-2</sup> )	Phase
165°E	0.11	308°	0.05	77°
175°E	0.03	263°	0.03	46°
175°W	0.04	239°	0.06	39°
165°W	0.06	224°	0.07	34°
155°W	0.06	153°	0.07	13°
145°W	0.08	122°	0.10	356°
135°W	0.05	113°	0.11	331°
125°W	0.09	72°	0.10	337°
115°W	0.08	55°	0.06	333°
105°W	0.07	34°	0.03	287°
95°W	0.04	342°	0.02	291°

a. Amplitude =  $a^2 + b^2$ , phase =  $\tan^{-1}(b/a)$ , and

$$\tau = \tau_0 + a_1 \cos \frac{2\pi}{12} t + b_1 \sin \frac{2\pi}{12} t + a_2 \cos \frac{2\pi}{6} t + b_2 \sin \frac{2\pi}{6} t.$$

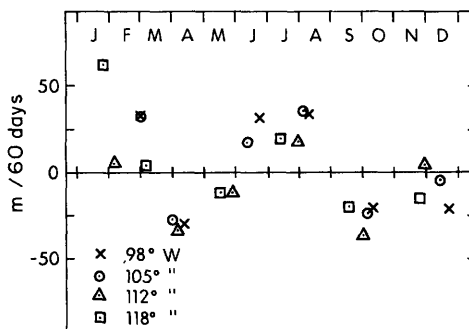


Figure 6.2 The rate at which the depth of the 20°C isotherm was observed to change during the EASTROPAC expedition in 1967 and early 1968.

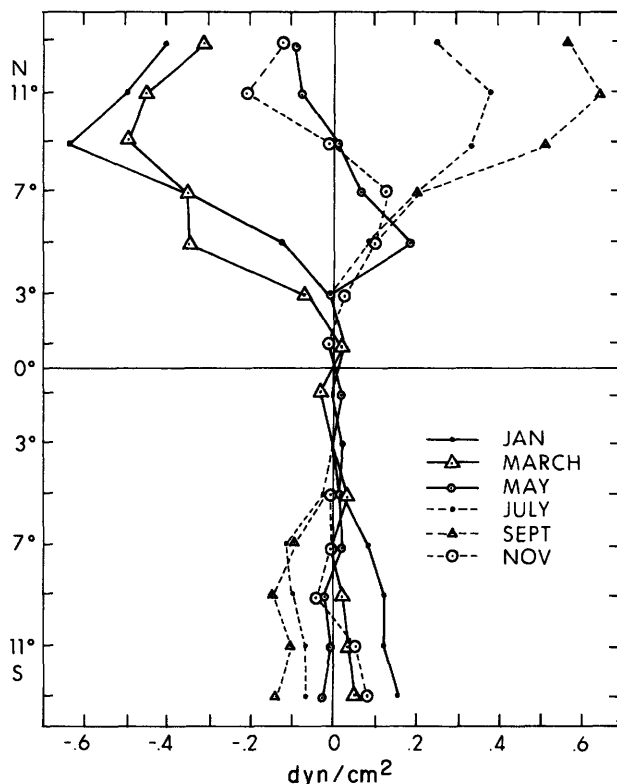


Figure 6.3 Profiles of zonal wind stress from 100 to 120°W, illustrating the annual cycle. To emphasize the meridional structure, the weak monthly mean value of the equatorial stress (the average of figures 6.1i and 6.1j) was subtracted from the monthly mean value at each latitude.

### 6.3 Theories

#### 6.3.1 Integrated Theories

The earliest theoretical attempts sought an explanation for the North Equatorial Countercurrent. This current defies intuition since it flows opposite to the prevailing winds. Montgomery and Palmén (1940) suggested that the easterly wind stress in the equatorial zone is balanced by the vertically integrated zonal pressure gradient. They presented supporting observational evidence in the Atlantic. One interesting result was their demonstration that the baroclinic pressure gradients generally were confined to the top few hundred meters of the water column. As an explanation for the North Equatorial Countercurrent, they hypothesized that in the doldrums, i.e., in the vicinity of the ITCZ, where the magnitude of the zonal stress is greatly reduced, the pressure gradient would maintain the value that it had on either side of this region and hence no longer be balanced by the wind stress. As a result, an eastward flow would develop, which they suggested would be retarded by lateral friction. Charts of dynamic topography (Tsuchiya, 1968) indicate that the zonal pressure gradient in this region is, in fact, less than it is farther to the north and south. Furthermore, since 1° or 2° off the equator Coriolis terms cannot be neglected and

the depth-integrated value of the meridional velocity usually does not vanish, the suggestion of Montgomery and Palmén (1940) does not represent a proper explanation for the North Equatorial Countercurrent.

Sverdrup (1947) suggested that the North Equatorial Countercurrent was not only a consequence of the zonal wind stress but also was related to the curl of the wind stress and continuity requirements. He assumed in his model that the currents were steady and vanished at a deep level. The equations were integrated from this depth to the sea surface; hence the solution gave no information about the vertical structure of the motion field. The apparent success of Sverdrup's theory in the eastern Pacific is often cited as observational endorsement of its widespread use in large-scale ocean-circulation theory.

In light of the earlier discussion about the large variability in the position and amplitude of the NECC, and the considerable monthly variation in the winds in this region, it is surprising that this steady theory should be applicable there. In fact, Sverdrup (1947) and Reid (1948), instead of using the mean wind stress in their computations, used the October–November values. They also used October–November oceanographic data to compute vertically integrated pressure. Implicit in their theory, then, was the assumption that the oceanic response to the fluctuating winds was sufficiently rapid that the ocean was almost always in equilibrium with the instantaneous winds (i.e., quasi-steady).

Therefore, it is of some interest to redo the computations of Sverdrup and Reid using the values for the monthly mean stress field from Wyrtki and Meyers (1975) and to compare the results with oceanographic data from different times of the year to see whether Sverdrup balance really is quasi-steady. The monthly values of the zonal Sverdrup transport are shown in figure 6.4. The October and November curves look quite similar to those of Sverdrup. The overall spatial and temporal evolution of the currents throughout the year resembles the picture that has been derived for the surface flow field from ship-drift observations. It is possible to check to see whether the historical integrated geostrophic transports follow a similar pattern of change.

During 1967 and the first part of 1968, hydrographic sections at four different longitudes between 100 and 120°W were occupied across the equator at seven different times. The geostrophic velocity computations relative to 500 db for these sections are given by Love (1972). Using these figures, the geostrophic transport for 2° bands of latitude from 2 to 12°N was computed by a planimetric integration. The minimum contour interval for the velocities was 5 cm s<sup>-1</sup>; this interval introduces an uncertainty of about 3 × 10<sup>9</sup> kg s<sup>-1</sup> into

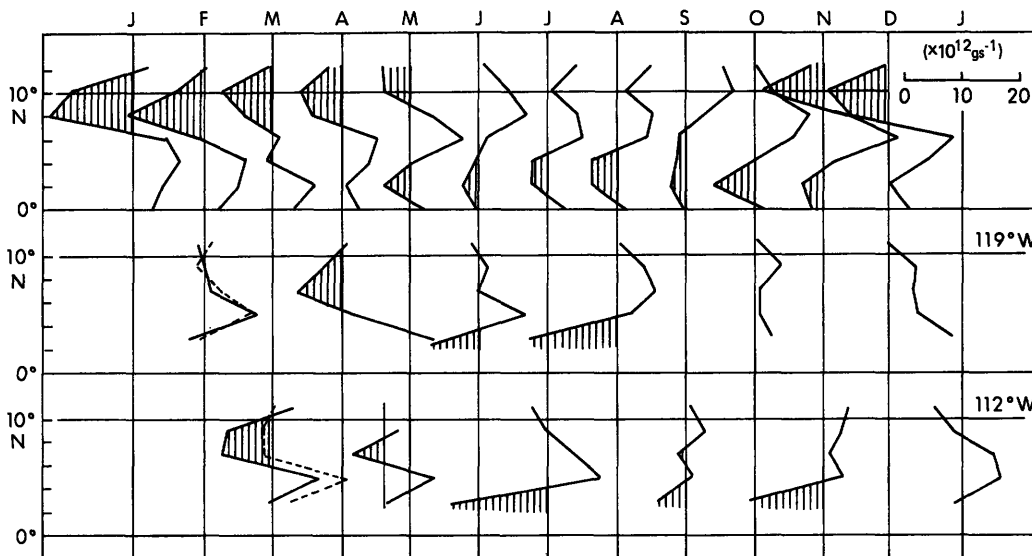


Figure 6.4 Upper panel depicts monthly Sverdrup transport. Lower two panels show geostrophic transports observed dur-

ing the EASTROPAC expedition.

each transport computation ( $2.5 \text{ cm s}^{-1} \times 500 \text{ m} \times 2^\circ \times 1 \text{ g cm}^{-3}$ ). The results of these integrations for the sections at  $119^\circ\text{W}$  and  $112^\circ\text{W}$  are shown in figure 6.4. The tendency at both sections is for the transport in the south equatorial current to be strongest during the summer. The NECC lies close to the equator early in the year and moves northward during the summer and southward again during late fall. The transport patterns at both sections during the first part of 1967 and 1968 are quite similar. This agreement could be coincidence or indicate that these fluctuations perhaps have a regular annual cycle. The observed geostrophic transport patterns are visually similar to the theoretical pattern; there clearly are quantitative differences, however.

The important conclusion from this study is that it cannot be said whether the Sverdrup relation provides an accurate description of the currents in the eastern tropical Pacific. Sverdrup and Reid were probably fortunate in that their results seemed to agree so well with observations. The real problem with testing Sverdrup theory, in light of what we now know about barotropic and baroclinic adjustment, is associated with the assumed level of no motion. For an ocean with a free-slip flat bottom, Sverdrup balance should hold for the integrated flows and pressures, as long as the integral goes all the way to the bottom and barotropic adjustment has had time to occur (approximately a few days). If the integration extends only over the surface layers (upper 500 or 1000 m, say), however, then the integrated quantities depend on both the barotropic and baroclinic components, and a quasi-steady theory will apply only if the dominant baroclinic modes have also reached equilibrium. In general for the annual cycle, there is no reason this should be true since baro-

clinic adjustment even near the equator takes at least a few months. Clearly what is needed is an understanding of baroclinic adjustment processes.

### 6.3.2 Baroclinic Theories

The discovery of the Equatorial Undercurrent in the Pacific in 1952 (Cromwell, Montgomery, and Stroup, 1954) triggered a great deal of equatorial modeling activity in the latter part of that decade. Almost all of these early models include baroclinic effects in a crude way by assuming the surface layer is essentially decoupled from the deep ocean below (Yoshida, 1959; Stommel, 1960; Charney, 1960). Another assumption common to these models is that all fields except the pressure are assumed to be independent of  $x$ , the east-west coordinate; the zonal pressure gradient  $\partial p / \partial x$  is taken to be a constant related to the zonal wind stress that is driving the motion.

The simplest and most elegant of these models is that of Stommel (1960). This model is the first successful extension of classical Ekman theory to the equator. Stommel's model equations balance the Coriolis force with vertical diffusion of momentum (the Ekman balance) while retaining horizontal pressure gradients. It is the zonal pressure gradient which allows him to avoid the equatorial singularity of previous Ekman theory, and which provides a source of eastward momentum to drive the undercurrent. The wind forcing is put into the ocean as a surface stress, and a zero-stress condition is imposed at the bottom of the layer. The vertical structure of the zonal velocity at the equator is parabolic, with surface flow in the direction of the wind and subsurface flow (undercurrent) in the opposite direction. In addition, the model develops a meridional circulation very similar to that hypothe-

sized by Cromwell to account for the distribution of tracers in the equatorial Pacific (Cromwell, 1953). Figure 6.5, by Stommel (1960), illustrates the circulation pattern developed by his model. There is surface divergence of fluid from the equator, subsurface convergence, and equatorial upwelling. A major drawback of this theory is that the response is too closely related to the choice of eddy viscosity  $\nu$ . Let  $U$  and  $L$  represent the velocity and depth scales of the flow and  $\tau$  measure the equatorial zonal wind stress. Let  $H$  be the depth of the layer and  $\beta$  be the meridional derivative of the Coriolis parameter. Then in the Stommel model

$$U = \frac{H\tau}{\nu} \quad \text{and} \quad L = \frac{\nu}{\beta H^2}. \quad (6.1)$$

It is not possible to select a value for  $\nu$  which simultaneously sets a realistic magnitude as well as width scale for the flow. In particular, if  $\nu$  is adjusted so that the current has a reasonable speed, then it is far too narrow.

Charney's (1960) nonlinear model differs fundamentally from Stommel's in that he requires a no-slip bottom boundary condition. Because of this stringent condition, the linear model cannot produce any flow counter to wind, and so it is clearly the presence of nonlinearities that allows the model to generate an undercurrent. Charney computed the zonal and vertical velocity only on the equator. Later, Charney and Spiegel (1971) extended the model off the equator to determine the flow field in a meridional section and also obtained the same general pattern of meridional circulation as that proposed by Cromwell. They explained the existence of an undercurrent in both models in the following qualitative manner [first suggested by Fofonoff and Montgomery (1955)]. Fluid converging toward the equator conserves absolute vorticity. As a result, planetary vorticity is converted to relative vorticity, and this conversion provides an additional source of eastward momentum to drive the

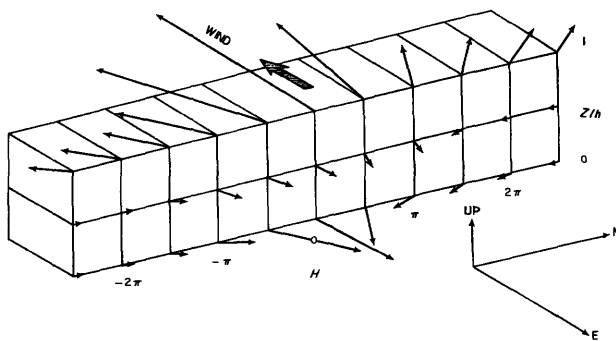


Figure 6.5 Schematic three-dimensional diagram of the flow field in the neighborhood of the equator, not showing the vertical component of velocity, which can in principle be determined from continuity. (After Stommel, 1960.)

undercurrent. These studies show that nonlinearities are likely to play an important role in equatorial dynamics. On the other hand, the nonlinear solutions are even more sensitive to the choice of  $\nu$  than Stommel's linear one. For example, when  $\nu$  decreases from 17 to 14  $\text{cm}^2 \text{s}^{-1}$ , the speed of the Equatorial Undercurrent more than doubles, and the  $e$ -folding width of the jet narrows significantly.

Other workers subsequently considered similar layer models and explored the importance of terms in the equations of motion that were ignored in the earlier studies (Philander, 1973; Cane, 1979b). Despite their successes, the layer models have obvious limitations. The assumption of an  $x$ -independent flow field is questionable, the decoupling of the lower layer is highly artificial, and the solutions are extremely dependent on the choice of mixing coefficients. Finally, the observations themselves suggest the most serious drawback. Although an undercurrent has been observed in the mixed layer (see for example Hisard, Merle, and Voituriez, 1970), the strongest eastward flow is almost always found in the thermocline below the surface mixed layer. Therefore, an undercurrent model that treats the effects of stratification in a more realistic way is required. It took another decade for such a model to be developed, and the development proceeded from an entirely different direction, namely, from attempts to understand time-dependent processes in the equatorial region.

Initial interest in equatorial waves was largely theoretical, and grew out of attempts to extend the theory of midlatitude gravity and Rossby waves to the equator. Longuet-Higgins (1964, 1965, 1968a) undertook a detailed investigation of planetary waves on a rotating sphere (cf. chapters 10 and 11). At about the same time, Blandford (1966) and Matsuno (1966) both used equatorial  $\beta$ -plane models (i.e., the Coriolis parameter is approximated by  $f = \beta y$ ) to describe free baroclinic waves. [Groves (1955) had earlier derived the same  $\beta$ -plane equatorially trapped solutions as Blandford and Matsuno, but he was considering barotropic tides.] All of these studies are linear and inviscid, and consider perturbations on a background state consisting of a stably stratified ocean at rest. Normal modes for the vertical structure of the fields are derived just as Fjeldstad (1933) originally did for internal waves. The eigenvalues for the vertical separation problem are usually presented as equivalent depths  $h'$  for the resulting normal modes. In general, for a finite depth ocean, there is one barotropic mode for which the equivalent depth is nearly equal to the actual depth of the ocean, and the corresponding eigenfunction describing the depth dependence of the horizontal velocities and pressure perturbation is nearly depth independent. There is also a denumerably infinite set of baroclinic equivalent

depths. The vertical structures of the baroclinic eigenfunctions depend on the details of the background density distribution. For each equivalent depth  $h'$ , there is a corresponding phase speed  $c$  defined by  $c^2 = gh'$ .

With this separation, the horizontal and time dependence of each vertical mode of the system can now be investigated independently of the  $z$ -dependence. If  $c$  is the phase speed for the mode in question, then free oscillations at frequency  $\omega$  can exist in a latitudinal band,  $|y| \leq y_T$ . In the equatorial  $\beta$ -plane model, the turning latitude is given by

$$y_T = \left( \frac{\omega^2}{\beta^2} + \frac{c^2}{4\omega^2} \right)^{1/2} \quad (6.2)$$

and is strongly dependent on  $\omega$ . For the first baroclinic mode,  $c$  is typically about  $250 \text{ cm s}^{-1}$ . Then at the annual cycle,  $y_T = 6250 \text{ km}$ ; at the 5-day period  $y_T = 640 \text{ km}$ , a much smaller trapping scale. [For a complete discussion of free equatorial trapped waves see Moore and Philander (1977) and chapter 10.]

Moore (1968) investigated the effects of oceanic boundaries on free waves at frequencies corresponding to strong equatorial trapping (near-minimum  $y_T$  for a given value of  $c$ ). He showed that a Kelvin wave at frequency  $\omega$  hitting an eastern boundary will generally reflect some of its energy back in the form of equatorially trapped Rossby waves, and the rest of the energy propagates poleward as coastally trapped Kelvin waves. These results were later extended to the case of an incoming Kelvin wave of step-function form by Anderson and Rowlands (1976a).

The first observational evidence—in Pacific sea-level variations—for the existence of strongly equatorially trapped baroclinic waves in the ocean was presented by Wunsch and Gill (1976). Spectral peaks corresponding to periods in the range 2–7 days were explained in terms of equatorially trapped inertial-gravity waves with vanishing east–west group velocity. The variation in the strength of the spectral peaks from islands at different latitudes was consistent with the expected latitudinal structure of the theoretical wave modes (see figure 10.11). Additional observational evidence for equatorially trapped waves was provided by Harvey and Patzert (1976) from deep mooring data in the eastern equatorial Pacific. Weisberg, Miller, Horigan, and Knauss (1980) and Weisberg, Horigan, and Colin (1979) did the same using Atlantic GATE data and later Gulf of Guinea observations.

An interesting property of the low-frequency large-scale baroclinic waves (nearly nondispersive Rossby waves) is that their phase speed increases markedly the more trapped they are to the equator. The swiftest wave, the equatorial Kelvin wave, is also the most strongly trapped. This property suggests that the forced

baroclinic response of the equatorial ocean need not remain locally confined to the forcing region, but can radiate swiftly away. That is to say, baroclinic effects may be remotely as well as locally forced.

In 1969, Lighthill published a seminal paper entitled “Dynamic Response of the Indian Ocean to the Onset of the Southwest Monsoon.” He was motivated by the idea that the Somali Current might be remotely forced by winds in the interior of the Indian Ocean. He coupled the wind stress to the model ocean in a novel way, not as a surface condition, but rather as a body force uniformly distributed throughout an upper mixed layer. This approach avoids the details of the frictional processes by which the stress actually enters the ocean and allows the use of the inviscid normal modes to study the oceanic response to variable wind forcing. The model ocean is forced by an impulsive wind-stress distribution concentrated away from the coast in the center of the Indian Ocean. In addition to the locally forced response, long-wavelength nondispersive Rossby waves are generated at the edge of the forcing region and propagate westward to the coast. They are reflected there as short-wavelength dispersive Rossby waves that remain trapped to the coast. He interpreted the coastal response as the onset of the Somali Current.

One of the most prominent features of the equatorial oceans is the presence of a strong near-surface pycnocline. Observations show that changes in the pycnocline depth can be large and occur very rapidly. It is sensible to model this motion as simply as possible, with either a one-and-a-half-layer model (a single upper moving layer overlying a slightly denser inert layer) or with a two-layer model; in both cases the layer interface plays the role of the pycnocline. Wind stress enters the ocean as a body force in the surface layer, and so such models are analogous to the Lighthill model if it is limited to a single baroclinic mode. Not surprisingly, a large number of these models, both linear and nonlinear, have been used in the past decade to investigate a variety of equatorial adjustment problems.

O’Brien and Hurlburt (1974) used a two-layer model to study the interior response of the equatorial Indian Ocean to change in zonal wind stress. The model produces an eastward equatorial jet with many of the observed features documented by Wyrtki (1973a). The meridional structure of the accelerating jet produced in the O’Brien and Hurlburt model is basically the same as the structure of the surface flow given in Yoshida’s (1959) undercurrent paper and has been called the Yoshida jet. See Moore and Philander (1977) for a detailed description of the spin-up of the Yoshida jet from rest for a single inviscid baroclinic mode.

The idea that the Somali Current might be remotely forced stimulated a number of additional studies. Anderson and Rowlands (1976b) used a one-and-a-half-



layer analytical model to investigate the relative importance of local and remote forcing. They concluded that local forcing is initially dominant but that remotely forced effects will ultimately become important. Hurlburt and Thompson (1976) used a two-layer model forced by a basin-wide northward stress  $\tau^y$  to show that nonlinear advective effects rapidly become important in the developing boundary flow. Cox (1976) addressed the same problem using a more sophisticated 12-level numerical model. His findings corroborate the conclusions of the simpler models.

Hickey (1975) and Wyrтки (1975b) suggested that El Niño occurs in conjunction with a relaxation of the southeast trades in the central and western Equatorial Pacific. Hurlburt, Kindle, and O'Brien (1976) applied substantially the same model as O'Brien and Hurlburt (1974) to simulate the onset of El Niño. They spun-up the model with a uniform westward wind for 50 days, and then turned off the wind. Major features of the response included an eastward-traveling Kelvin wave originating at the western boundary, westward-traveling nondispersive Rossby waves originating at the eastern boundary, and poleward-traveling Kelvin waves along the eastern boundary. The thickening of the warm layer near the eastern boundary in response to the relaxation of the winds demonstrated the plausibility of Wyrтки's hypothesis. Although the model of Hurlburt, Kindle, and O'Brien was nonlinear, the response was completely dominated by linear dynamics. The only discernible nonlinear effect was the steepening front of the poleward-propagating coastal Kelvin wave.

McCreary (1976) used a one-and-a-half-layer linear model in a similar study of El Niño. He followed the initial response of the eastern ocean to various zonally uniform distributions of wind stress. Important conclusions are the following. Changes in the meridional wind field cannot cause an El Niño event. Changes in the zonal wind field outside the equatorial band (roughly  $\pm 5^\circ$  of latitude) are not important in generating El Niño. Finally, model results suggest that the meridional profile of the wind field can significantly affect the resulting flow field. For example, the southward motion of the ITCZ can force southward cross-equatorial transport of water in the eastern Pacific. It is interesting that in this model the deepening of the pycnocline in the eastern Pacific is initiated by the weakening of the local zonal winds, and is stopped by the arrival of an equatorially trapped Kelvin wave from the western ocean.

McCreary (1977, 1978), realizing that the changes in the Pacific wind field during El Niño are not zonally uniform, but rather are confined in the central and western ocean, extended the model of the 1976 study so that a wind-stress patch of limited longitudinal ex-

tent could be imposed. Figure 6.6 shows the adjustment of the model thermocline topography after a weakening of the westward trade winds by an amount  $+0.5 \text{ dyn cm}^{-2}$ . The dotted lines in the upper left panel of the figure delineate the region of weakened trade winds; the wind-stress change is a maximum in the central portion and weakens markedly in the surrounding areas. After 35 days, a downwelling signal rapidly radiates from the region of the wind patch as a packet of equatorially trapped Kelvin waves and already the equatorial thermocline (and also sea level) begins to tilt to generate a zonal pressure gradient that balances the wind there. In the region of strongest wind curl, the thermocline begins to move closer to the surface, and this upwelling signal propagates westward as a packet of Rossby waves. After 69 days, the packet of Kelvin waves has already reflected from, and spread along, the eastern boundary. As time passes, this downwelling signal propagates back into the ocean interior as a packet of Rossby waves, and more and more upper-layer water piles up in the eastern ocean. As shown in the lower two panels, the source of the water is a broad area of the western and central ocean where the thermocline is uplifted; in some regions the thermocline rises over 65 m. Note that in this case it is the arrival of the Kelvin wave that causes the initial deepening of the pycnocline in the eastern ocean. The figure also further demonstrates the importance of knowing the horizontal structure of the wind field; the rapid tilting of the equatorial thermocline, and the form of the extraequatorial upwelling are a direct result of the particular structure chosen here.

Moore et al. (1978) suggested that the equatorial upwelling in the eastern Atlantic and coastal upwelling in the Gulf of Guinea might be a remote response to an increase in the strength of the westward wind stress in the western Atlantic. The variation of  $\partial p / \partial x$  in the western Atlantic reported by Katz et al. (1977) was interpreted as the response to such an increase. O'Brien, Adamec, and Moore (1978) and Adamec and O'Brien (1978) used the same basic adjustment model as had been applied earlier to the Indian and Pacific Oceans to study Atlantic adjustment. The ocean geometry is rectangular with a rectangular notch cut out of the northeast corner of the basin to simulate West Africa. The model calculations showed that an increase in strength of the westward wind stress in the western Atlantic generates an equatorial-upwelling response that propagates eastward, leaving behind a thermocline tilt to balance the stress. When it hits the coast, the upwelling signal propagates away from the equator along the boundary and travels westward along the coast of the Gulf of Guinea.

The important role that equatorially trapped waves play in all these models has stimulated several studies

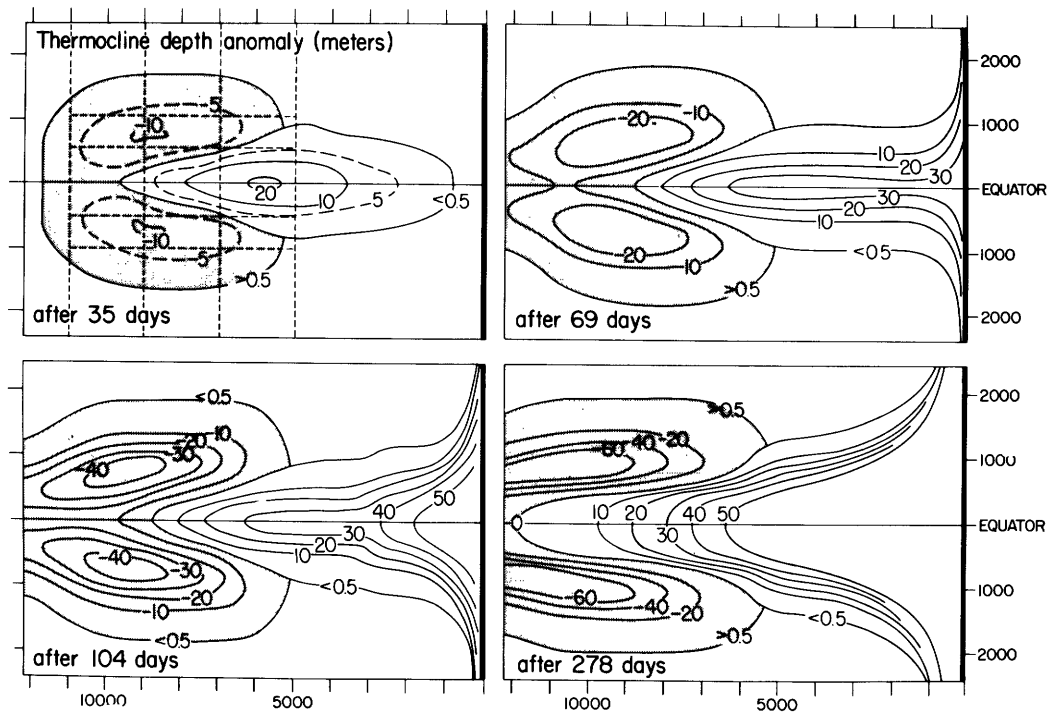


Figure 6.6 Time development of the thermocline depth anomaly to a longitudinally confined zonal wind stress. The dotted lines in the upper left panel indicate the region of the

wind. The solid lines in each panel indicate the presence of an eastern ocean boundary. Horizontal distances are in kilometers. (After McCreary, 1977.)

of the interaction of the waves with the mean zonal currents. Hallock (1977) used a two-and-a-half-layer model forced by meridional surface winds to investigate the Equatorial Undercurrent meanders observed during GATE. A meridional stress  $\tau^y$  with a zonal wavelength of 2400 km is turned on gradually in a few days and then held steady. Part of the response is an equatorially trapped Yanai wave of about 16-day period. The characteristics of this Yanai wave were somewhat, but not drastically, modified by including mean surface currents in the upper layer and a mean undercurrent in the second layer. Thus it was suggested that the GATE observations of Equatorial Undercurrent meanders might be explained in terms of passive advection of the Equatorial Undercurrent by a wind-generated Yanai wave. McPhaden and Knox (1979) and Philander (1979) used one-and-a-half-layer models to study the modifications of other free waves in the presence of various meridional profiles of zonal mean currents. McPhaden and Knox concentrate on the equatorial Kelvin and inertial-gravity waves (including the Yanai wave), and conclude that the zonal velocity associated with a given mode can be strongly modified by the background currents. Philander also considers equatorial Rossby waves and suggests that these waves may be influenced strongly by the presence of the Equatorial Undercurrent.

Philander (1976) used a two-and-a-half-layer model to show that background zonal currents also allow unstable waves and predicted a possible instability of the surface currents in the tropical Pacific. The most unstable waves which propagate westward have a wavelength of about 1000 km and a period of approximately 25 days. The satellite observations of Legeckis (1977b) seem consistent with the instability scales Philander predicted. A later numerical study by Cox (1980) confirmed a suggestion of Philander's that oscillations generated by such surface-current instabilities could propagate zonally for large distances while propagating vertically into the deep ocean. The results indicate that the Harvey and Patzert (1976) observations in the eastern Pacific near the sea floor could, in fact, be such remote effects of surface-current instabilities generated farther to the west.

It is now apparent that simple layer models have been remarkably successful in reproducing many of the obvious features of time-dependent equatorial ocean circulation. These models are intrinsically limited, however, in their ability to describe the vertical structure of the ocean, and recently theoreticians have begun to study more sophisticated models that allow for high vertical resolution. There are several reasons for this interest. In 1975, Luyten and Swallow (1976) discovered high-vertical-wavenumber equatorially trapped multiple jets in the Indian Ocean, and in 1978 similar structures were observed in the Pacific (C. Erik-

sen, personal communication). In addition to this observational impetus, general theoretical questions arise in trying to understand in greater detail just how the wind stress enters the ocean. For example, how valid is the assumption that the wind enters as a body force distributed over a surface mixed layer? Finally, there is the perennial interest in understanding the dynamics of the Equatorial Undercurrent.

In order to model the multiple jets, Wunsch (1977) considered an inviscid continuously stratified model, which he took to be horizontally unbounded and infinitely deep. (At the end of his study he also reported effects introduced by a western ocean boundary.) Since the model was inviscid, it was not possible to introduce the wind stress as a surface boundary condition. Instead, Wunsch assumed that a thin wind-driven surface boundary layer pumped the deeper ocean with a surface distribution of vertical velocity. For convenience, he chose for the form of the distribution a westward-propagating sinusoidal wave. To specify the solution, he required it to match this vertical velocity distribution at the ocean surface and also to exhibit upward phase propagation everywhere in the upper ocean (a radiation condition). Although the north-south scale of the imposed surface  $w$ -field was broad, the significant response was strongly equatorially trapped and showed an oscillatory structure in the vertical, just as in the observations.

In an effort to understand better how wind stress enters the equatorial ocean and to explore further the vertical structures that might be possible in stratified viscid equatorial oceans, Moore (unpublished) has studied the simplest linear model that includes the effects of continuous stratification and vertical mixing on an equatorial  $\beta$ -plane. The buoyancy frequency  $N$  is taken as constant, constant eddy coefficients for vertical mixing of heat  $\kappa$  and momentum  $\nu$  are used, and, for convenience, unit Prandtl number is assumed ( $\nu = \kappa$ ). The ocean is laterally unbounded and infinitely deep. The simplest problem to treat is the analog of the Yoshida jet, in which the system is driven by a uniform zonal wind stress  $\tau$  started impulsively at  $t = 0$ . The problem as posed has a natural or canonical scaling. This means that for suitable choices of velocity scale  $U$ , time scale  $T$ , horizontal length scale  $L$ , and depth scale  $H$ , the resulting nondimensional equations contain no parameters. The scales are

$$\begin{aligned} L &= (\nu N^2 / \beta^3)^{1/2}, \\ T &= (\nu \beta^2 N^2)^{-1/5}, \\ H &= (\nu^2 / \beta N)^{1/5}, \\ U &= \tau (\beta N \nu^3)^{-1/5}. \end{aligned} \tag{6.3}$$

Note that equations (6.3) are much less dependent on  $\nu$  than are equations (6.1), essentially because here the depth scale is no longer an externally set constant! This weak dependency on  $\nu$  is a characteristic advantage that all stratified models have over their homogeneous counterparts. For  $N = 2 \times 10^{-3} \text{ s}^{-1}$ ,  $\nu = 20 \text{ cm}^2 \text{ s}$ , and  $\tau = 1 \text{ dyn cm}^{-2}$ , the typical values are  $L = 60 \text{ km}$ ,  $T = 8 \text{ days}$ ,  $H = 40 \text{ m}$ , and  $U = 2 \text{ m s}^{-1}$ . Figures 6.7A–6.7C show  $\{y, z\}$ -profiles of the zonal velocity  $u$  at times  $t = 0.25, 1.0,$  and  $5.0$  in Moore's model (the equator is at the right). The ranges are  $0 \leq y \leq 5$  positive to the left and  $0 \leq z < 10$  positive down. Right on the equator in this  $x$ -independent model, the zonal velocity is simply governed by downward diffusion of momentum:  $u_t = \nu u_{zz}$ . The contour plot at time  $t = 0.25$  shows that initially this balance is nearly true everywhere. At later times, the Coriolis effects have a distinct influence on the solution. The equatorial jet is well developed by  $t = 1$ . The solution serves to illustrate typical time and space scales of equatorial processes, as well as to point out their dependence on model parameters. Moreover, the model clearly suggests that the diffusion of zonal momentum into the deep ocean may play an important role in equatorial dynamics. However, in this  $x$ -independent and bottomless model the jet continues to intensify and deepen indefinitely. The only way to reach a steady state is to require a non-slip bottom on the ocean or to allow zonal pressure gradients, either by adding zonal structure to the wind field or by introducing boundary effects.

In the past 2 years, several fully three-dimensional and continuously stratified ocean models have been used to study wind-driven equatorial ocean circulation. The numerical models of Semtner and Holland (1980) and Philander and Pacanowski (1980a,b) are nonlinear. The analytical model of McCreary (1980) is linear; it can be regarded as an extension of the Lighthill model that allows the diffusion of heat and momentum into the deeper ocean, and also as an extension of the Stommel model into a stratified ocean. All three models are remarkably successful in reproducing many of the observed features of the Equatorial Undercurrent. For example, figure 6.8 [taken from McCreary (1980)] shows the flow field in the center of the ocean basin (10,000 km wide), where the zonal wind stress reaches a maximum ( $-0.5 \text{ dyn cm}^{-2}$ ). The model Equatorial Undercurrent is situated in the main thermocline beneath a surface mixed layer (75 m). The width and depth scales, as well as the speed, of the zonal flow are realistic. In addition, the pattern of meridional circulation resembles quite well the classic pattern suggested by Cromwell (1953); note that there is a strong convergence of fluid slightly above the core of the Equatorial Undercurrent, strong surface upwelling, and weaker downwelling below the core. The presence of

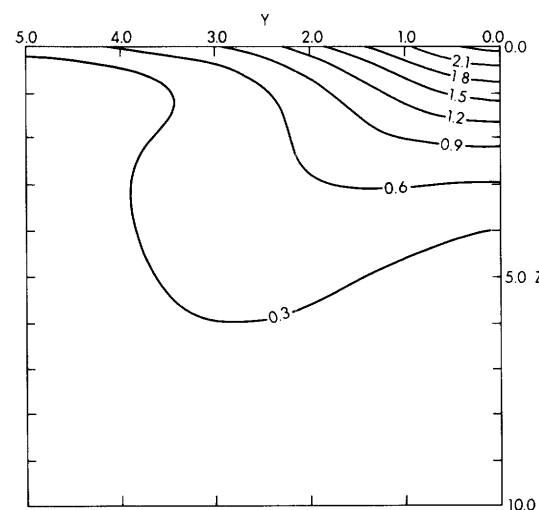
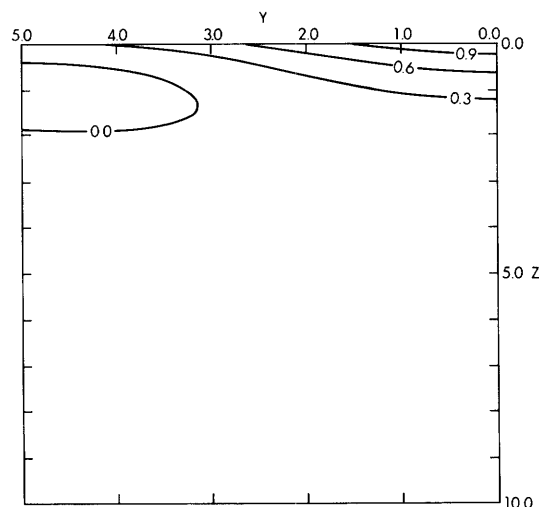
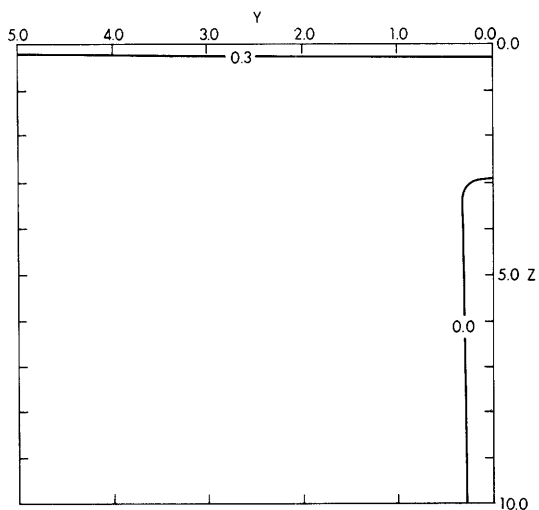


Figure 6.7  $(y, z)$ -contour plots of zonal velocity  $u$  in  $x$ -independent stratified spin-up on an equatorial  $\beta$ -plane, including the effects of vertical mixing. (A)  $t = 0.25$ . Diffusion effects are dominant. (B)  $t = 1.0$ . Equatorial jet starts to develop. (C)  $t = 5.0$ . Jet continues to deepen.

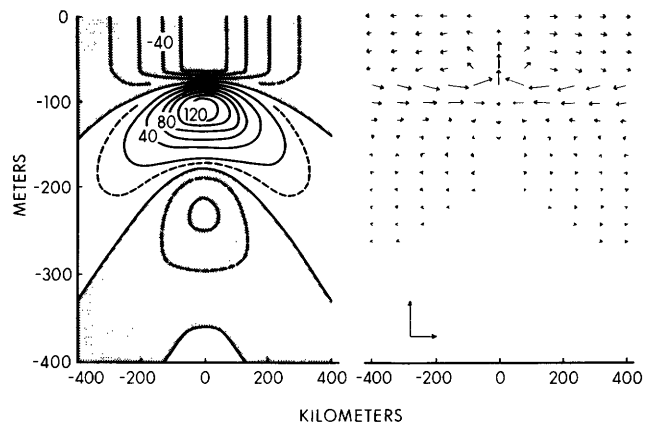


Figure 6.8 Vertical sections of zonal velocity (left panel) and meridional circulation (right panel) at the center of the ocean basin. The contour interval is  $20 \text{ cm s}^{-1}$ ; dotted contours are  $\pm 10 \text{ cm s}^{-1}$ . Calibration arrows in the lower left corner of the right panel have amplitudes  $0.005 \text{ cm s}^{-1}$  and  $10 \text{ cm s}^{-1}$ , respectively. (After McCreary, 1980.)

zonal baroclinic pressure gradients and the diffusion of momentum into the deep ocean are crucial for the development of this undercurrent. In fact, at the equator the balance of terms is simply  $p_x = (\nu u_z)_z$ . Just as in the  $x$ -independent model discussed in the preceding paragraph, stratification weakens considerably the dependence of the solution on  $\nu$ . It is this property that allows a realistic undercurrent to be generated for a wide range of choices of  $\nu$ . The success of the linear model suggests that nonlinearities are not essential for maintaining the Equatorial Undercurrent. They apparently act only to modify the linear dynamics, not to destroy it.

#### 6.4 Discussion

Observations of the equatorial oceans during the past 30 years have shown the existence of surprisingly strong subsurface currents and greatly increased our knowledge of the mean structure and time variability of the surface flows. Zonal currents, both surface and subsurface, tend to occur as narrow jets several hundred kilometers wide, several hundred meters deep, and thousands of kilometers long. The observations also suggest that many tropical ocean events are remotely forced. A prime example is the phenomenon of El Niño, where wind changes in the central and western Pacific are associated with strong changes in the thermal structure of the eastern Pacific.

Perhaps because the signal-to-noise ratio is so large, theoreticians have had remarkable success in providing explanations for many equatorial phenomena. All the models suggest that stratification is an essential ingredient in equatorial dynamics. Width, depth, and time scales of model response are all intimately related to

the background buoyancy frequency distribution [e.g., see equation (6.3)]. The presence of stratification also allows the existence of swiftly propagating equatorially trapped baroclinic waves. These waves have been used to account for remotely forced events as well as the meandering of equatorial currents.

Additional experimental and theoretical work needs to be done. It is now known that the tropical ocean responds readily and coherently to large-scale low-frequency changes in the wind field. Moreover, the nature of the response depends critically on the spatial distribution of the wind field. It is important, then, to monitor the detailed structure of the wind field on the seasonal, annual, and interannual time scales. For the first time, such observations may be practical due to rapidly improving satellite technology. Long time series of the variability of the tropical ocean flow field must also be obtained. Equatorial observations made in 1979 as part of the Global Weather Experiment should add substantial new knowledge about the circulation in all three equatorial oceans. However, the duration of this experiment is too short; it will provide at most a single realization of the annual cycle.

A major advance in our understanding of equatorial dynamics occurred when simple layer models began to be studied. These models were successful because their solutions could be easily and convincingly compared with observations; the layer interface is interpretable as the motion of the pycnocline. The recent use of equatorial models with high vertical resolution suggests that other advances may soon be forthcoming. Such models can produce a much more detailed picture of the flow field, and so can be quantitatively compared to a greater degree with the observations. Obvious problems to which these models should be applied include the existence of the thermostat and the associated subsurface countercurrents and the presence of multiple jet structures at the equator. In addition, even more sophisticated models that include realistic surface mixed layers need to be developed.